




Is Digital Breast Tomosynthesis Superior to Digital Mammography? A Preclinical Evaluation of Tumor Histopathological Markers Using Digital Breast Tomosynthesis

Aysegul Altunkeser¹, Zeynep Fatma Arslan ^{2*}, Mehmet Ali Eryilmaz³, Muslu Kazım Korez⁴ and Zeynep Bayramoğlu⁵

¹Department of Radiology, Konya Training and Research Hospital, University of Health Science, Konya, Turkey

²Department of Radiology, Basaksehir City Hospital, Istanbul, Turkey

³Department of General Surgery, Konya Training and Research Hospital, University of Health Science, Konya, Turkey

⁴Department of Statistics, Faculty of Science, Selcuk University, Konya, Turkey

⁵Department of Pathology, Konya Training and Research Hospital, University of Health Science, Konya, Turkey

*Corresponding author: Department of Radiology, Basaksehir City Hospital, Istanbul, Turkey. Email: zeynep_a1002@hotmail.com

Received 2021 February 23; Revised 2021 September 04; Accepted 2021 September 05.

Abstract

Background: Digital mammography (DM) and digital breast tomosynthesis (DBT) are important radiological modalities, which increase the survival of breast cancer patients. Breast cancer is a morphologically heterogeneous disease with various histopathological parameters and multiple receptors in its biological profile.

Objectives: This study aimed to analyze the morphological features of invasive breast cancer on DM and DBT, to investigate the contribution of DBT to DM, to examine the association of DBT findings with pathological molecular subtypes, Bloom-Richardson grade, and Ki-67 index, and to determine the effect of breast parenchyma density on the relationship between DBT findings and hormone receptors.

Patients and Methods: A total of 36 patients with malignant lesions were evaluated in this study. According to the American College of Radiology (ACR) classification, the lesion features were divided into subgroups based on DM and DBT, and the findings were compared. The relationships between DBT findings and the hormone receptor status, molecular classification, and Bloom-Richardson grade were also investigated, and the effect of density on these relationships was assessed.

Results: The mean age of the patients ($n = 36$) was 53 years. Based on the comparison of DM and DBT findings, spiculated margins, mass density, architectural distortion, and microcalcifications were significantly more frequent in DBT. Lesions with indistinct margins on DM were observed as mass lesions with spiculated margins on DBT ($P < 0.001$). Regarding the relationship between DBT findings and hormone receptor status and Ki-67 proliferation index, in progesterone receptor (PR)-positive patients, an irregular tumor shape was more common (89.7%). In PR-negative patients, skin changes and nipple retraction were more frequently seen ($P = 0.03$ for skin changes, and $P = 0.049$ for nipple retraction). Regarding the association between Bloom-Richardson grade (BRG) and DBT findings, tumors with a higher grade were more likely to be associated with a high tumor density ($P = 0.032$). Also, considering the relationship between molecular classification and DBT findings, skin changes and nipple retraction were significantly more frequent in triple-negative masses compared to other subtypes ($P = 0.011$ for skin changes and $P = 0.016$ for nipple retraction).

Conclusion: DBT is superior to DM, as it reveals the lesion margins, density, and architectural distortion more accurately. The majority of PR-positive tumors were irregular, while most PR-negative cases were round. The mass density also increased as the tumor grade increased. Skin change and nipple retraction were frequently seen in triple-negative tumors compared to other subtypes. Therefore, DBT is a promising diagnostic tool for showing molecular subtypes in dense breasts.

Keywords: Breast Cancer, Doppler Ultrasonography, Digital Mammography System, Tomosynthesis

1. Background

Digital mammography (DM) is the most important radiological screening and diagnostic tool, which has been shown to increase the survival of breast cancer patients (1). While the sensitivity of DM is high in fatty breasts,

it decreases to 30% in dense breasts (2). In DM, dense fibroglandular tissue may lead to false negative results by superimposing on the lesion margins (2). To eliminate superimposing the normal fibroglandular tissue, an adjunctive radiological method, such as ultrasonography or

digital breast tomosynthesis (DBT), is commonly applied. DBT is a recently developed modality that yields multiple mammographic images and combines them with an algorithm to create a three-dimensional image. By allowing the breast tissue examination in different sections, DBT decreases the superimposition of fibroglandular tissue and improves the detection rate of breast cancer significantly (3).

Breast cancer is a morphologically heterogeneous disease with various histopathological parameters and multiple receptors in its biological profile. Differences in the gene expression profile of breast tumors may be responsible for differences in the prognosis of patients. In the latest edition of breast tumor classification by the World Health Organization (WHO), it has been declared that breast cancer is heterogeneous at the molecular level (4). Estrogen receptors (ER), progesterone receptors (PR), human epidermal growth factor receptor 2 (HER2), and Ki-67 antigen are commonly used for the molecular classification of breast tumors. Currently, five widely accepted molecular subgroups have been identified: (1) luminal A; (2) luminal B, HER2-positive; (3) luminal B, HER2-negative; (4) HER2 positive; and (5) triple negative (5).

Major efforts have been made, especially in the last few years, to classify breast tumors at the molecular level and find more effective treatments (6). Besides, detection of breast cancer molecular subtypes using radiological modalities is of particular importance for the early treatment of breast cancer. Therefore, early detection and treatment can provide long-term survival advantages (7). Although many studies have investigated the relationship between the morphological features of tumors detected by DM and the molecular subgroups of breast cancer, few studies have examined the relationships between lesion subgroups in DBT, which is a more effective modality for dense breasts.

2. Objectives

This study aimed to analyze the morphological features of invasive breast cancer on DM and DBT, to investigate the contribution of DBT to DM, to examine the association of DBT findings with the pathological molecular subtypes, Bloom-Richardson grade (BRG), and Ki-67 index, and finally, to investigate the effect of breast parenchyma density on the relationship between DBT findings and hormone receptor status.

3. Patients and Methods

A total of 36 patients with histopathologically proven malignant lesions were evaluated in this study. The

histopathological results were obtained using Tru-cut biopsy or mastectomy. The exclusion criteria were as follows: (1) undergoing surgery or biopsy; (2) having other formerly known malignancies; and (3) receiving neoadjuvant chemotherapy.

The pathological subgroups and BRG were based on the fifth edition of the WHO guidelines. The luminal A subtype was defined as ER positivity, PR positivity, low Ki-67 index, and if applicable, multigene expression and low risk of recurrence. Although the luminal B, HER2-negative subtype was defined as being ER positive and HER2 negative, it was associated with a high Ki-67 index, low or negative PR, multigene expression, and a high recurrence risk. Moreover, in the luminal B, HER2-positive subtype, ER positivity and HER2 overexpression or amplification are essential. Also, the luminal B, HER2-positive subtype is defined as a high Ki-67 index and PR receptor positivity. In the HER2-positive subtype, the overexpression or amplification of HER2 and loss of ER and PR are essential. Finally, the triple-negative subtype is characterized by negative ER, PR, and HER2. In this classification system, a high Ki-67 index is defined as $\geq 20\%$, and ER and PR positivity is defined as 1%.

All patients underwent DM and DBT. A commercially available device (Mammomat Inspiration, Siemens, Erlangen, Germany) was used for all DM examinations. Also, DBT images were acquired using a Giotto Breast Tomosynthesis System (IMS, Bologna, Italy). The DM and DBT images were available in our local database. Mammography (MG) followed by DBT was performed for the patients. The patients' images were evaluated by two radiologists, one of whom was specialized in breast radiology.

The breast density was classified as a, b, c, and d on MG. This classification was based on the 2013 American College of Radiology (ACR) breast atlas (8). There were two main categories of breast tissue: (1) non-dense (a and b); and (2) dense (c and d). According to the ACR classification, the shape of masses was divided into oval, round, and irregular. The margin features of the lesions were designated as circumscribed, obscured, microlobulated, indistinct, and spiculated. Also, the lesion density was determined as high density, isodensity, and low density in each modality (DM and DBT).

Moreover, the presence of microcalcifications was investigated in this study. If there was any microcalcification, it was divided into groups of typically benign (punctate) and suspicious morphology (amorphous, coarse heterogeneous, fine pleomorphic, and fine linear or branching), according to the microcalcification morphology. Besides, the microcalcification distribution was divided into categories of regional, grouped, linear, and segmental.

Additionally, architectural distortion, intramammary lymph nodes, skin changes, and nipple retraction were as-

sessed in the present study. Tumor size, number of microcalcifications, and number of foci (foci with similar characteristics, but located in different points from the main lesion) were determined for each modality. Each of these previously measured morphological features was first evaluated by DM and then DBT, and the DM and DBT findings were compared. Moreover, the relationship between DBT findings and hormone receptor status was investigated, and the effect of density was assessed. Also, the relationship between DBT findings and molecular classification and BRG was determined.

This study was conducted based on the ethical standards, outlined in the Declaration of Helsinki of the World Medical Association (WMA). The study protocol was approved by our institutional review board. The study was carried out after an institutional ethical clearance was obtained.

3.1. Statistical Analysis

All statistical analyses were performed in R 3.6.0 (www.r-project.com). The Anderson-Darling test and Q-Q plot were used to examine the normal distribution of data. Continuous variables are presented as mean \pm standard deviation (minimum/maximum) and compared using Student's *t*-test. Categorical variables are described as number (n) and percentage (%) and compared using chi-square test. Moreover, to determine the superiority of DBT to DM, the interval likelihood ratio, sensitivity, and specificity were calculated. Besides, alluvial plots were drawn to show the distribution of PR subtypes in dense breasts according to skin changes, mass shape, and nipple retraction. A P-value less than 0.05 was considered statistically significant.

4. Results

The mean age of the patients (n=36) was 53 years. Overall, 63% of the patients had lesions in the left breast, and 66.7% of the patients showed a dense parenchymal pattern. ER was positive in 31 (86.1%) patients, PR was positive in 29 (80.6%) patients, and HER2 was negative in 20 (55.6%) patients. Based on the findings, in 20 (55.6%) patients, the Ki-67 index was ≥ 20 . According to the BRG system, 18 (50%) patients were classified as grade 3, and four patients were in the unclassified group. As for the molecular classification, luminal B, HER2-positive subtype was detected in 11 (30.6%) patients; it was the most commonly seen subgroup in the present study (Table 1).

Based on the comparison of DM and DBT findings, spiculated margins, tumor density, architectural distortion, and microcalcifications were significantly higher in DBT. The mass lesion with indistinct margins on DM was seen as

Table 1. The Clinical and Pathological Features of Breast Cancer on DBT^a

Characteristics	Number of breasts (percentage)
Age (y), mean \pm SD (min - max)	53.94 \pm 9.08 (35 - 75)
Side	
Right	13 (36.1)
Left	23 (63.9)
Density pattern	
B	12 (33.3)
C	21 (58.3)
D	3 (8.3)
Breast density	
Non-dense	12 (33.3)
Dense	24 (66.7)
ER	
Negative	5 (13.9)
Positive	31 (86.1)
PR	
Negative	7 (19.4)
Positive	29 (80.6)
HER2	
Negative	20 (55.6)
Positive	16 (44.4)
Ki-67 index	
Low (< 20%)	16 (44.4)
High ($\geq 20\%$)	20 (55.6)
BRG	
Grade 1	2 (5.6)
Grade 2	12 (33.3)
Grade 3	18 (50)
No grading (not possible)	4 (11.1)
Molecular classification	
Luminal A subtype	8 (22.2)
Luminal B subtype, HER2+	11 (30.6)
Luminal B subtype, HER2-	6 (16.7)
HER2+	2 (5.6)
Triple-negative subtype	3 (8.3)
No molecular classification	6 (16.7)

Abbreviations: ER, estrogen receptor; PR, progesterone receptor; HER2, human epidermal growth factor receptor 2; BRG, bloom-Richardson grading system.

^a Values are expressed as number of breasts (%) unless otherwise indicated.

a lesion with spiculated margins on DBT ($P < 0.001$) (Figure 1A and B). Spiculated margins, high density, and architectural distortions were strong predictors of malignant tumors in DBT, as the likelihood ratio was 3.63 (1.92 - 6.82), 2.14 (1.38 - 3.31), and 1.39 (1.06 - 1.83), respectively, and sensitivity was estimated at 80.5, 83.3, and 88.8%, respectively. The majority of masses showed high densities on DBT ($P < 0.001$). The detection rate of architectural distortions on DBT was significantly higher than DM ($P = 0.013$). DBT was superior to DM in displaying the number of microcalcifications and satellite foci; however, the difference was not statistically significant (Table 2 and Figure 2).

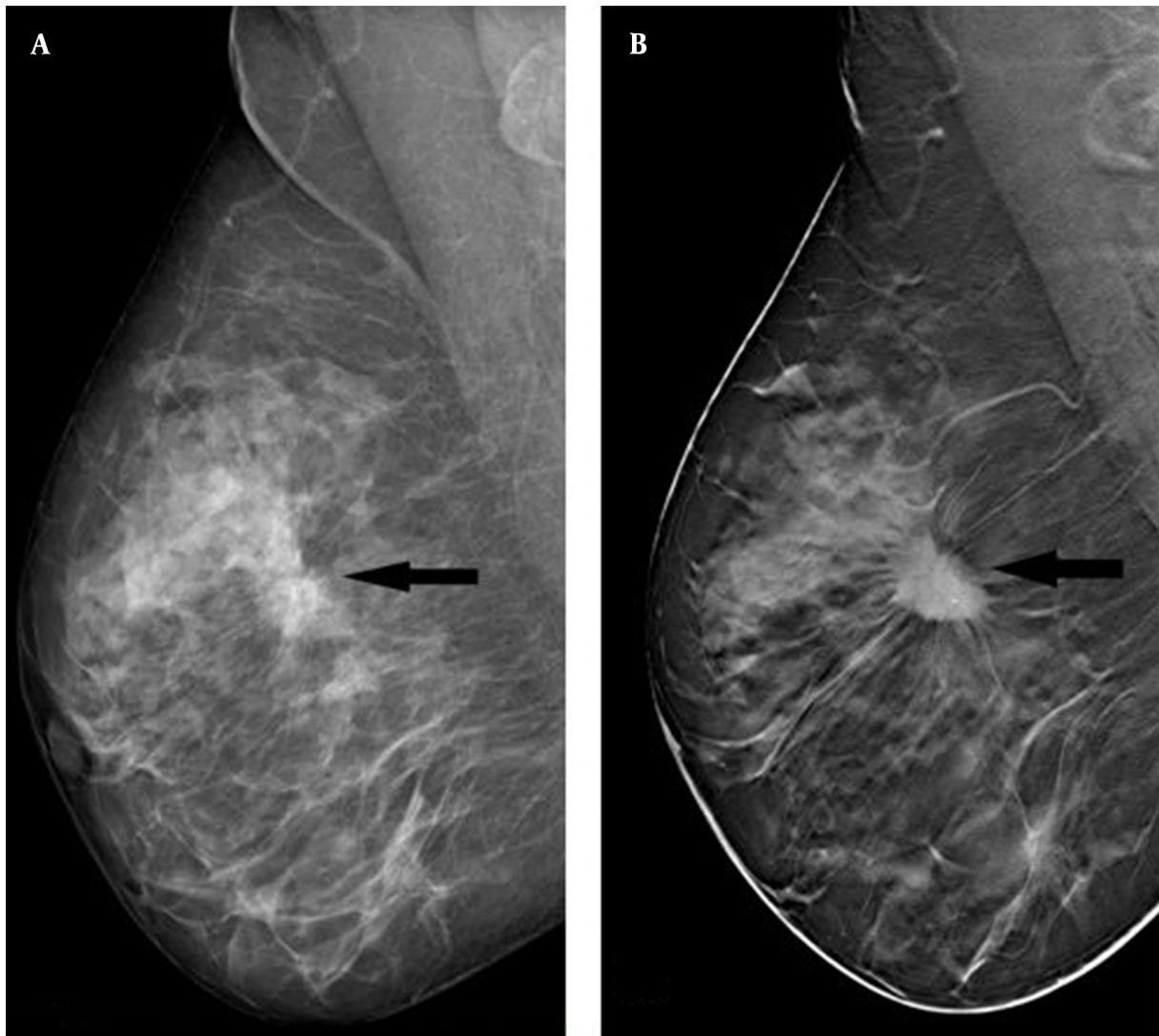


Figure 1. The mediolateral oblique view (A) reveals a lesion (arrow) in the middle quadrant of the right breast. The lesion margin is indistinct on digital mammography (DM). In the digital breast tomosynthesis (DBT) (B), the lesion margin is more visible and appears spiculated (arrow).

Regarding the association of DBT findings with the hormone receptor status and Ki-67 proliferation index, an irregular mass shape was mostly observed in PR-positive patients (89.7%), while a round mass shape was more common in PR-negative patients (57%) ($P = 0.003$). In PR-negative patients, skin changes and nipple retraction were more frequent compared to PR-positive patients ($P = 0.03$ for skin changes and $P = 0.049$ for nipple retraction). However, no significant association was found between DBT findings and other receptors or Ki-67 proliferation index (Table 3). Regarding the effect of density on the significant relationship between the PR status and DBT findings, a significant relationship was only found in the dense group (P

$= 0.006$ for mass shape; $P = 0.038$ for skin changes; and $P = 0.038$ for nipple retraction). Nevertheless, no significant correlation was found in the non-dense group.

In the dense group, 5.6% of PR-positive patients had round-shaped tumors, while 94% of them had irregular tumors. In the dense group, 66.7% of PR-negative patients had round tumors, whereas 33.3% of them had irregular ones. While skin changes and nipple retraction were observed in 66.7% of PR-negative patients in the dense group, 83.3% of PR-positive patients did not show such findings (Table 4). The figurative alluvial plots of this table are presented below (Figure 3A - C).

Regarding the association of BRG with DBT findings, a

Table 2. Comparison of DM and DBT Findings According to the Morphological Features ^{a, b, c, d}

Variables	MG (n = 36)	DBT (n = 36)	Total	P-Value
Mass shape				ns
Oval	1 (2.8)	1 (2.8)	2 (2.8)	
Round	12 (33.3)	7 (19.4)	19 (26.4)	
Irregular	23 (63.9)	28 (77.8)	51 (70.8)	
Mass margin				< 0.001
Circumscribed	1 (2.8)	0 (0)	1 (1.4)	
Obscured	6 (16.7)	0 (0)	6 (8.3)	
Microlobulated	3 (8.3)	2 (2)	5 (6.9)	
Indistinct	18 (50) ^A	5 (13.9) ^B	23 (31.9)	
Spiculated	8 (22.2) ^A	29 (80.6) ^B	37 (51.4)	
Density				< 0.001
High density	14 (38.9) ^A	30 (83.3) ^B	44 (61.1)	
Isodensity	21 (58.3) ^A	6 (16.7) ^B	27 (37.5)	
Low density	1 (2.8)	0 (0)	1 (1.4)	
Microcalcification				0.002
No	23 (63.9) ^A	10 (27.8) ^B	33 (45.8)	
Yes	13 (36.1) ^A	26 (72.2) ^B	39 (54.2)	
Calcification morphology				ns
Punctate	2 (12.5)	1 (4.5)	3 (7.9)	
Amorphous	11 (68.8)	16 (72.7)	27 (71.1)	
Pleomorphic	3 (18.8)	5 (22.7)	8 (21.1)	
Distribution of microcalcifications				ns
Regional	2 (12.5)	3 (13.6)	5 (13.2)	
Grouped	11 (68.8)	16 (72.7)	27 (71.1)	
Linear	0 (0)	2 (9.1)	2 (5.3)	
Segmental	3 (18.8)	1 (4.5)	4 (10.5)	
Architectural distortion				0.013
No	13 (36.1) ^A	4 (11.1) ^B	17 (23.6)	
Yes	23 (63.9) ^A	32 (88.9) ^B	55 (76.4)	
Intramammary lymph nodes				ns
No	32 (88.9)	27 (75)	59 (81.9)	
Yes	4 (11.1)	9 (25)	13 (18.1)	
Skin changes				ns
No	28 (77.8)	28 (77.8)	56 (77.8)	
Yes	8 (22.2)	8 (22.2)	16 (22.2)	
Nipple retraction				ns
No	27 (75)	27 (75)	54 (75)	
Yes	9 (25)	9 (25)	18 (25)	
Tumor diameter, mean ± SD	22.17 ± 13.67	25.08 ± 12.17		ns
Number of microcalcifications	7.72 ± 12.09	10.97 ± 13.03		0.276
Number of foci	0.22 ± 0.59	0.92 ± 1.36		0.007

Abbreviations: SD, standard deviation; ns, not significant; DM, digital mammography; DBT, digital breast tomosynthesis; MG, Mammography.

^a Values are expressed as No. (%) unless otherwise indicated.

^b Each capital letter (A - B) denotes a significantly different proportion.

^c P-values are calculated by chi-square test and Student's *t*-test.

^d *p* < 0.05 is considered statistically significant.

significant relationship was found only between the mass density and grade. Accordingly, tumors with higher grades were more likely to be accompanied by a high density (*P*

= 0.032). Considering the association of BRG with other DBT findings, no significant difference was detected (Table 5). Besides, regarding the relationship between molecu-

Table 3. The Relationship Between DBT Findings and Hormone Receptor Status and Ki-67 Index

Variables	ER		PR		HER2		Ki-67 index	
	-(n=5)	+(n=31)	-(n=7)	+(n=29)	-(n=20)	+(n=16)	Low (n=16)	High (n=20)
Mass shape								
Oval	0 (0)	1 (3.2)	1 (14.3)	0 (0)	0 (0)	1 (6.3)	0 (0)	1 (5)
Round	3 (60)	4 (12.9)	4 (57.1)	3 (10.3)	5 (25)	2 (12.5)	3 (18.8)	4 (20)
Irregular	2 (40)	26 (83.9)	2 (28.6)	26 (89.7)	15 (75)	13 (81.3)	13 (81.3)	15 (75)
P-value	ns		0.003		ns		ns	
Mass margin								
Microlobulated	0 (0)	2 (6.5)	0 (0)	2 (6.9)	1 (5)	1 (6.3)	1 (6.3)	1 (5)
Indistinct	0 (0)	5 (16.1)	1 (14.3)	4 (13.8)	1 (5)	4 (25)	2 (12.5)	3 (15)
Spiculated	5 (100)	24 (77.4)	6 (85.7)	23 (79.3)	18 (90)	11 (68.8)	13 (81.3)	16 (80)
P-value	ns		ns		ns		ns	
Density								
High density	5 (100)	25 (80.6)	7 (100)	23 (79.3)	16 (80)	14 (87.5)	12 (75)	18 (90)
Isodensity	0 (0)	6 (19.4)	0 (0)	6 (20.7)	4 (20)	2 (12.5)	4 (25)	2 (10)
P-value	ns		ns		ns		ns	
Microcalcifications								
No	2 (40)	8 (25.8)	3 (42.9)	7 (24.1)	4 (20)	6 (37.5)	2 (12.5)	8 (40)
Yes	3 (60)	23 (74.2)	4 (57.1)	22 (75.9)	16 (80)	10 (62.5)	14 (87.5)	12 (60)
P-value	ns		ns		ns		ns	
Calcification morphology								
Punctate	1 (33.3)	0 (0)	1 (25)	0 (0)	0 (0)	1 (8.3)	0 (0)	1 (8.3)
Amorphous	2 (66.7)	14 (73.7)	3 (75)	13 (72.2)	7 (70)	9 (75)	8 (80)	8 (66.7)
Pleomorphic	0 (0)	5 (26.3)	0 (0)	5 (27.8)	3 (30)	2 (16.7)	2 (20)	3 (25)
P-value	ns		ns		ns		ns	
Distribution of microcalcifications								
Regional	1 (33.3)	2 (10.5)	2 (50)	1 (5.6)	1 (10)	2 (16.7)	1 (10)	2 (16.7)
Grouped	2 (66.7)	14 (73.7)	2 (50)	14 (77.8)	8 (80)	8 (66.7)	8 (80)	8 (66.7)
Linear	0 (0)	2 (10.5)	0 (0)	2 (11.1)	0 (0)	2 (16.7)	0 (0)	2 (16.7)
Segmental	0 (0)	1 (5.3)	0 (0)	1 (5.6)	1 (10)	0 (0)	1 (10)	0 (0)
P-value	ns		ns		ns		ns	
Architectural distortion								
No	0 (0)	4 (12.9)	1 (14.3)	3 (10.3)	2 (10)	2 (12.5)	3 (18.8)	1 (5)
Yes	5 (100)	27 (87.1)	6 (85.7)	26 (89.7)	18 (90)	14 (87.5)	13 (81.3)	19 (95)
P-value	ns		ns		ns		ns	
Intramammary lymph nodes								
No	5 (100)	22 (71)	7 (100)	20 (69)	16 (80)	11 (68.8)	14 (87.5)	13 (65)
Yes	0 (0)	9 (29)	0 (0)	9 (31)	4 (20)	5 (31.3)	2 (12.5)	7 (35)
P-value	ns		ns		ns		ns	
Skin changes								
No	2 (40)	26 (83.9)	3 (42.9)	25 (86.2)	14 (70)	14 (87.5)	11 (68.8)	17 (85)
Yes	3 (60)	5 (16.1)	4 (57.1)	4 (13.8)	6 (30)	2 (12.5)	5 (31.3)	3 (15)
P-value	ns		0.030		ns		ns	
Nipple retraction								
No	2 (40)	25 (80.6)	3 (42.9)	24 (82.8)	14 (70)	13 (81.3)	11 (68.8)	16 (80)
Yes	3 (60)	6 (19.4)	4 (57.1)	5 (17.2)	6 (30)	3 (18.8)	5 (31.3)	4 (20)
P-value	ns		0.049		ns		ns	

Abbreviations: Ns, not significant; ER, estrogen receptors; PR, progesterone receptor; HER2, human epidermal growth factor receptor 2.

^a Values are described as number of breasts (%).^b P-values are calculated by chi-square test.^c P < 0.05 is considered statistically significant.

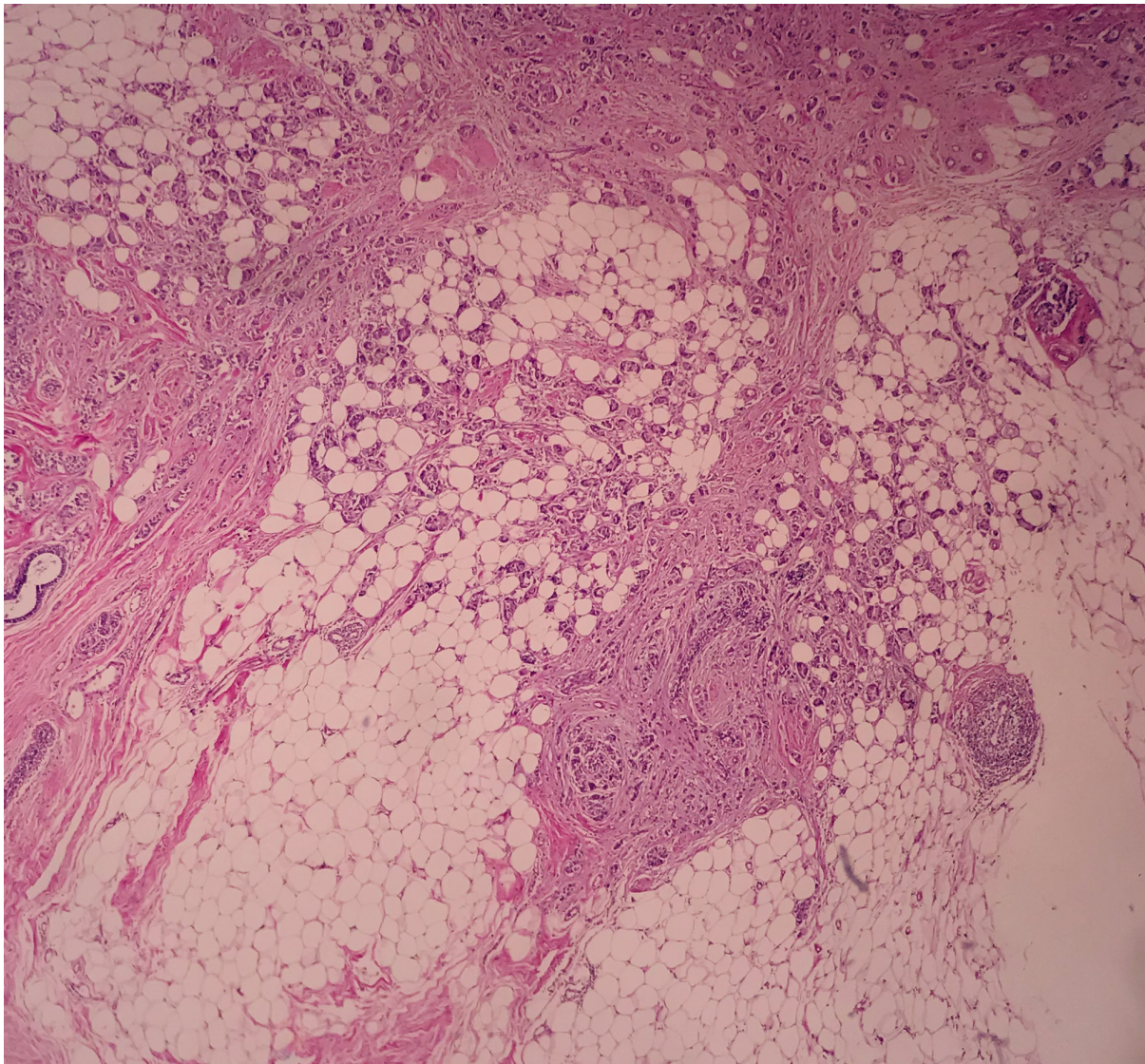


Figure 2. A stained breast slide with hematoxylin-eosin (H&E) at 40× magnification. Invasive breast carcinoma invades the adipose tissue and forms a gland structure.

lar classification and DBT findings, skin changes and nipple retraction were significantly more frequent in triple-negative masses compared to other subtypes ($P = 0.011$ for skin changes and $P = 0.016$ for nipple retraction). In other subtypes, no significant difference was detected (Table 6).

5. Discussion

DM is the modality of choice for screening and diagnosis of breast cancer. Since a malignant lesion can be observed in a single section, and the contours of normal breast tissue overlap with the lesion, mammographic sen-

sitivity and tumor visibility may decrease due to poor visualization in dense breast tissue, with a false negativity rate of 8 to 66% (9). Therefore, integration of DBT into DM can increase the radiologists' confidence, especially in dense breasts, and help detect the lesion borders more accurately (10).

It is important to determine morphological features, such as tumor density, margin, shape, and microcalcification for distinguishing benign lesions from malignant ones (11). The present study, which investigated the superior features of DBT to DM, revealed that DBT visualized the spiculated margins and high-density features of malig-

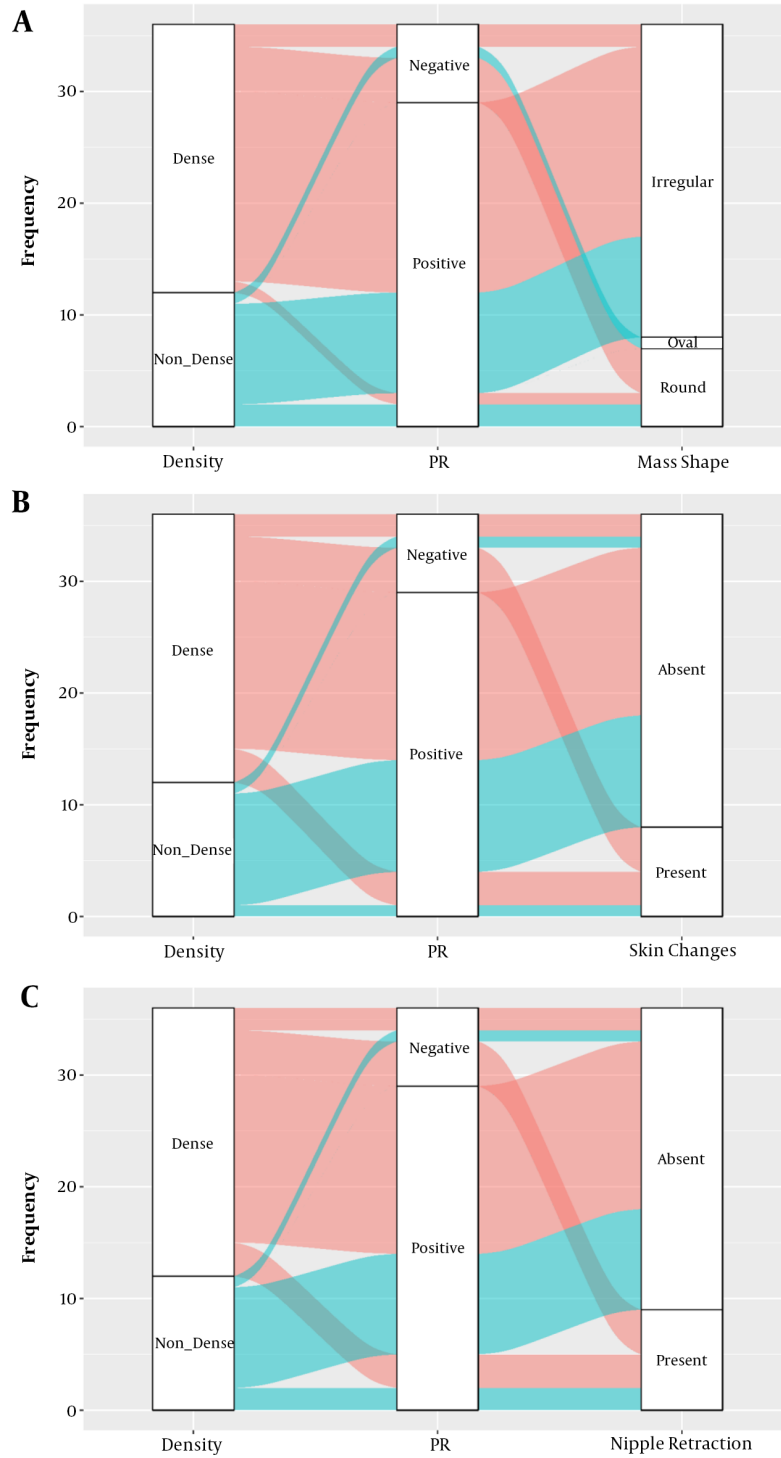


Figure 3. A, Mass shape; B, Skin change; and C, Nipple retraction are alluvial plots according to the dynamics of breast density and progesterone receptor (PR) receptor status. The pink color represents the dense parenchyma, and the green color represents non-dense breast parenchyma.

Table 4. The Effect of Breast Density on the Relationship Between the PR Receptor Status and Mass Shape, Skin Changes, and Nipple Retraction^{a, b, c}

Variables	Non-dense breasts		Dense breasts	
	PR- (n = 1)	PR+ (n = 11)	PR- (n = 6)	PR+ (n = 18)
Mass shape				
Oval	1 (100)	0 (0)	-	-
Round	0 (0)	2 (18.2)	4 (66.7)	1 (5.6)
Irregular	0 (0)	9 (81.8)	2 (33.3)	17 (94.4)
P-value	ns		0.006	
Skin changes				
No	1 (100)	10 (90.9)	2 (33.3)	15 (83.3)
Yes	0 (0)	1 (9.1)	4 (66.7)	3 (16.7)
P-value	ns		0.038	
Nipple retraction				
No	1 (100)	9 (81.8)	2 (33.3)	15 (83.3)
Yes	0 (0)	2 (18.2)	4 (66.7)	3 (16.7)
P-value	ns		0.038	

Abbreviations: ns, not significant; PR, progesterone receptor.

^a Values are described as No. (%).

^b P-values are calculated by chi-square test.

^c P < 0.05 is considered statistically significant.

nant masses more clearly. Moreover, DBT displayed structural distortions, microcalcifications, and foci more accurately than DM. In this regard, Rangarajan et al. reported that DBT is useful in the detection of architectural distortions, visualizing the lesion margins clearly by eliminating tissue overlaps (12).

Although detection of malignant calcifications associated with a small tumor size (barely visible lesions) facilitates mammographic diagnosis, it is very difficult to detect these lesions without calcifications on DM, especially in dense breasts. Evidence suggests that almost 23% of these barely visible malignant lesions are overlooked in DM (13). In another study, DM was insufficient in showing foci and staging compared to DBT, and more lesions were found in 10% of patients by integrating DBT into DM compared to DM alone (14). Therefore, DBT can be a useful modality for mass definition and microcalcification detection in dense breasts, as seen in the majority of our patients.

Molecular classification is important for the prediction of prognosis and effective treatment of breast cancer. The survival rates and treatment options for breast cancer vary depending on subtypes (15). With the detection of various hormone receptors, Ki-67 index, and histological subtypes, aggressiveness of a tumor can be estimated (6). A previous study explained that patients with HER2-enriched tumors have higher rates of nodal involvement, multifocality, intraductal components, and lymphovascular invasion compared to those with luminal A tumors (16).

Recent evidence suggests that radiological appearance may be associated with the molecular subtype and help identify the biological behavior of breast cancer (17, 18).

Previous research has investigated the relationship between DM and pathological subtypes (19). However, few studies have investigated the relationship between DBT and pathological subtypes. In this regard, Sartor et al. reported a higher mammographic density in ER-negative tumors, which indicated a poor prognosis compared to other subtypes in a study using DM (20). In our study using DBT, a significant association was found between the tumor grade and density. It is known that malignant masses have higher densities, which may indicate high-grade breast cancer.

Liu et al. revealed a significant relationship between the luminal A subtype and spiculated margins of tumors on DM. They also reported that a lower Ki-67 index and HER2 negativity might be the most important contributors to a spiculated mass (18). Similar to this study, the relationships between morphological features and receptor status, tumor grade, and pathological subgroups on DBT, which is superior to DM in terms of mass definition, were examined in the current study. It was found that spiculated contours were common in ER- and PR-positive groups, and the masses were generally irregular in PR-positive patients.

In line with previous findings (18), ER and PR positivity and HER2 negativity could cause spiculated contours in a mass in the present study. Besides, skin changes and nipple retraction were higher in PR-negative tumors compared to PR-positive tumors. Overall, previous studies have reported significant differences between morphological features and subtypes on DBT. The findings show that DBT can demonstrate the lesion margins, microcalcifications, and lymph nodes more accurately. Besides, the HER2 over-

Table 5. The Association Between Bloom-Richardson Grade (BRG) and DBT Findings^{a, b, c}

Variables	BRG grade				Total	P-value
	Grade 1	Grade 2	Grade 3	Grade cannot be determined		
Mass shape						ns
Oval	0 (0)	1 (8.3)	0 (0)	0 (0)	1 (2.8)	
Round	0 (0)	1 (8.3)	5 (27.8)	1 (25)	7 (19.4)	
Irregular	2 (100)	10 (83.3)	13 (72.2)	3 (75)	28 (77.8)	
Mass margin						ns
Microlobulated	0 (0)	1 (8.3)	0 (0)	1 (25)	2 (5.6)	
Indistinct	0 (0)	1 (8.3)	3 (16.7)	1 (25)	5 (13.9)	
Spiculated	2 (100)	10 (83.3)	15 (83.3)	2 (50)	29 (80.6)	
Density						0.032
High density	0 (0)	11 (91.7)	16 (88.9)	3 (75)	30 (83.3)	
Isodensity	2 (100)	1 (8.3)	2 (11.1)	1 (25)	6 (16.7)	
Microcalcification						ns
No	0 (0)	4 (33.3)	6 (33.3)	0 (0)	10 (27.8)	
Yes	2 (100)	8 (66.7)	12 (66.7)	4 (100)	26 (72.2)	
Calcification morphology						ns
Punctate	0 (0)	0 (0)	1 (8.3)	0 (0)	1 (4.5)	
Amorphous	1 (100)	5 (83.3)	7 (58.3)	3 (100)	16 (72.7)	
Pleomorphic	0 (0)	1 (16.7)	4 (33.3)	0 (0)	5 (22.7)	
Distribution of microcalcifications						ns
Regional	0 (0)	0 (0)	3 (25)	0 (0)	3 (13.6)	
Grouped	1 (100)	6 (100)	6 (50)	3 (100)	16 (72.7)	
Linear	0 (0)	0 (0)	2 (16.7)	0 (0)	2 (9.1)	
Segmental	0 (0)	0 (0)	1 (8.3)	0 (0)	1 (4.5)	
Architectural distortion						ns
No	1 (50)	1 (8.3)	1 (5.6)	1 (25)	4 (11.1)	
Yes	1 (50)	11 (91.7)	17 (94.4)	3 (75)	32 (88.9)	
Intramammary lymph nodes						ns
No	1 (50)	9 (75)	13 (72.2)	4 (100)	27 (75)	
Yes	1 (50)	3 (25)	5 (27.8)	0 (0)	9 (25)	
Skin changes						ns
No	2 (100)	9 (75)	13 (72.2)	4 (100)	28 (77.8)	
Yes	0 (0)	3 (25)	5 (27.8)	0 (0)	8 (22.2)	
Nipple retraction						ns
No	2 (100)	10 (83.3)	11 (61.1)	4 (100)	27 (75)	
Yes	0 (0)	2 (16.7)	7 (38.9)	0 (0)	9 (25)	

Abbreviation: Ns, not significant; DBT, digital breast tomosynthesis.

^a Values are expressed as No. (%).

^b P-values are calculated using chi-square test.

^c P < 0.05 is considered statistically significant.

expression subtype was associated with a larger tumor size and more microcalcifications compared to the luminal B subtype on DBT (21). Conversely, a recent prospective population-based study demonstrated no significant difference between DM and DBT in terms of histological subtypes (22). In our study, the frequency of skin changes and nipple retraction was significantly higher in triple-negative tumors compared to other subtypes; in triple-

negative tumors with a poor prognosis, this may be an indicator of tumor aggressiveness.

In the present study, regarding the relationship between molecular subtypes and DBT findings, the majority of patients had dense breasts, and significant differences were found between PR-positive and PR-negative dense breasts in terms of mass shape, nipple retraction, and skin changes. While the majority of PR-positive masses in dense

Table 6. The Relationship Between Molecular Classification and DBT Findings^{a, b, c}

Variables	Molecular classification						P-value
	Luminal A subtype	Luminal B subtype, HER2+	Luminal B subtype, HER2-	HER2+	Triple-negative subtype	No molecular classification	
Mass shape							ns
Oval	0 (0)	1 (9.1)	0 (0)	0 (0)	0 (0)	0 (0)	
Round	0 (0)	1 (9.1)	1 (16.7)	1 (50)	2 (66.7)	2 (33.3)	
Irregular	8 (100)	9 (81.8)	5 (83.3)	1 (50)	1 (33.3)	4 (66.7)	
Mass margin							ns
Microlobulated	0 (0)	0 (0)	1 (16.7)	0 (0)	0 (0)	1 (16.7)	
Indistinct	0 (0)	3 (27.3)	0 (0)	0 (0)	0 (0)	2 (33.3)	
Spiculated	8 (100)	8 (72.7)	5 (83.3)	2 (100)	3 (100)	3 (50)	
Density							ns
High density	6 (75)	10 (90.9)	5 (83.3)	2 (100)	3 (100)	4 (66.7)	
Isodensity	2 (25)	1 (9.1)	1 (16.7)	0 (0)	0 (0)	2 (33.3)	
Microcalcification							ns
No	0 (0)	5 (45.5)	2 (33.3)	1 (50)	1 (33.3)	1 (16.7)	
Yes	8 (100)	6 (54.5)	4 (66.7)	1 (50)	2 (66.7)	5 (83.3)	
Calcification morphology							ns
Punctate	0 (0)	0 (0)	0 (0)	1 (100)	0 (0)	0 (0)	
Amorphous	3 (60)	6 (75)	2 (66.7)	0 (0)	2 (100)	3 (100)	
Pleomorphic	2 (40)	2 (25)	1 (33.3)	0 (0)	0 (0)	0 (0)	
Distribution of microcalcifications							ns
Regional	0 (0)	2 (25)	0 (0)	0 (0)	1 (50)	0 (0)	
Grouped	4 (80)	4 (50)	3 (100)	1 (100)	1 (50)	3 (100)	
Linear	0 (0)	2 (25)	0 (0)	0 (0)	0 (0)	0 (0)	
Segmental	1 (20)	0 (0)	0 (0)	0 (0)	0 (0)	0 (0)	
Architectural distortion							ns
No	1 (12.5)	1 (9.1)	0 (0)	0 (0)	0 (0)	2 (33.3)	
Yes	7 (87.5)	10 (90.9)	6 (100)	2 (100)	3 (100)	4 (66.7)	
Intramammary lymph nodes							ns
No	6 (75)	6 (54.5)	4 (66.7)	2 (100)	3 (100)	6 (100)	
Yes	2 (25)	5 (45.5)	2 (33.3)	0 (0)	0 (0)	0 (0)	
Skin changes							0.011
No	5 (62.5)	9 (81.8)	6 (100)	2 (100)	0 (0)	6 (100)	
Yes	3 (37.5)	2 (18.2)	0 (0)	0 (0)	3 (100)	0 (0)	
Nipple retraction							0.016
No	5 (62.5)	8 (72.7)	6 (100)	2 (100)	0 (0)	6 (100)	
Yes	3 (37.5)	3 (27.3)	0 (0)	0 (0)	3 (100)	0 (0)	

Abbreviations: Ns, not significant; ER, estrogen receptors; PR, progesterone receptors; HER2, human epidermal growth factor receptor 2; DBT, digital breast tomosynthesis.

^a Values are described as number of breasts (%).

^b P-values are calculated using chi-square test.

^c P < 0.05 is considered statistically significant.

breasts had an irregular shape, most of the lesions were round-shaped, which is frequent in PR-negative tumors. On the other hand, in PR-negative tumors, skin changes and nipple retraction were more frequent; there was no significant difference in non-dense breasts. Therefore, DBT can be a useful tool for predicting the PR receptor status of

masses, especially in dense breasts.

There were some limitations to our study. First, it was conducted on a relatively small sample size. Second, during the evaluations, interobserver variability could not be assessed, because the two radiologists reached a common consensus.

In conclusion, DBT was found to be superior to DM, as it could visualize the lesion margins, mass density, and architectural distortions more accurately. The majority of PR-positive tumors were irregular, while the majority of PR-negative tumors were round-shaped. Besides, the mass density increased as the tumor grade advanced. Skin changes and nipple retraction were more common in triple-negative tumors compared to other subtypes. Therefore, DBT may be used as a potential diagnostic tool that can show molecular subtypes in dense breasts. Further comprehensive studies are needed to reveal the morphological features of breast cancer subgroups.

Footnotes

Authors' Contribution: Study conception and design, A.A. and F.Z.A.; Acquisition of data, A.A. and F.Z.A.; Analysis and interpretation of data, K.K.; Drafting of the manuscript, F.Z.A.; Critical revision of the manuscript for important intellectual content, A.A.; Statistical analysis, K.K.; Administrative, technical, and material support, Z.B.; and Study supervision, M.A.E.

Conflict of Interests: The authors declare that there is no conflict of interest.

Ethical Approval: Ethical approval was obtained from the local ethics committee of Konya Training and Research Hospital (05/03/2020; No: 36-28).

Funding/Support: This research did not receive any specific grant from any funding agencies in the public, commercial, or not-for-profit sectors.

Informed Consent: This was a retrospective study based on the data obtained from a local database. It was carried out retrospectively years after the patients' online records were registered. Therefore, it was not possible to find the patients and ask them for consent.

References

- Garcia M, Jemal AW, Ward EM, Center MM, Hao Y, Siegel RL, et al. *Breast cancer facts & figures*. Atlanta, USA: American Cancer Society; 2007.
- Mohindra N, Neyaz Z, Agrawal V, Agarwal G, Mishra P. Impact of addition of digital breast tomosynthesis to digital mammography in lesion characterization in breast cancer patients. *Int J Appl Basic Med Res*. 2018;**8**(1):33-7. doi: [10.4103/ijabmr.IJABMR_372_16](https://doi.org/10.4103/ijabmr.IJABMR_372_16). [PubMed: [29552533](https://pubmed.ncbi.nlm.nih.gov/29552533/)]. [PubMed Central: [PMC5846217](https://pubmed.ncbi.nlm.nih.gov/PMC5846217/)].
- Sprague BL, Coley RY, Kerlikowske K, Rauscher GH, Henderson LM, Onega T, et al. Assessment of radiologist performance in breast cancer screening using digital breast tomosynthesis vs digital mammography. *JAMA Netw Open*. 2020;**3**(3). e201759. doi: [10.1001/jamanetworkopen.2020.1759](https://doi.org/10.1001/jamanetworkopen.2020.1759). [PubMed: [32227180](https://pubmed.ncbi.nlm.nih.gov/32227180/)]. [PubMed Central: [PMC7292996](https://pubmed.ncbi.nlm.nih.gov/PMC7292996/)].
- Lakhani SR; International Agency for Research on Cancer; World Health Organization. *WHO Classification of Tumours of the Breast*. Lyon, France: International Agency for Research on Cancer; 2012.
- Falck AK, Ferno M, Bendahl PO, Ryden L. St Gallen molecular subtypes in primary breast cancer and matched lymph node metastases—aspects on distribution and prognosis for patients with luminal A tumours: Results from a prospective randomised trial. *BMC Cancer*. 2013;**13**:558. doi: [10.1186/1471-2407-13-558](https://doi.org/10.1186/1471-2407-13-558). [PubMed: [24274821](https://pubmed.ncbi.nlm.nih.gov/24274821/)]. [PubMed Central: [PMC4222553](https://pubmed.ncbi.nlm.nih.gov/PMC4222553/)].
- Paquet ER, Hallett MT. Absolute assignment of breast cancer intrinsic molecular subtype. *J Natl Cancer Inst*. 2015;**107**(1):357. doi: [10.1093/jnci/dju357](https://doi.org/10.1093/jnci/dju357). [PubMed: [25479802](https://pubmed.ncbi.nlm.nih.gov/25479802/)].
- Liedtke C, Kiesel L. Breast cancer molecular subtypes—modern therapeutic concepts for targeted therapy of a heterogeneous entity. *Maturitas*. 2012;**73**(4):288-94. doi: [10.1016/j.maturitas.2012.08.006](https://doi.org/10.1016/j.maturitas.2012.08.006). [PubMed: [23020990](https://pubmed.ncbi.nlm.nih.gov/23020990/)].
- American College of Radiology. *Atlas breast imaging reporting and data system*. Reston, USA: American College of Radiology; 2013.
- Asbeutah AM, Karmani N, Asbeutah AA, Echreshzadeh YA, AlMajran AA, Al-Khalifah KH. Comparison of digital breast tomosynthesis and digital mammography for detection of breast cancer in Kuwaiti women. *Med Princ Pract*. 2019;**28**(1):10-5. doi: [10.1159/000495753](https://doi.org/10.1159/000495753). [PubMed: [30476905](https://pubmed.ncbi.nlm.nih.gov/30476905/)]. [PubMed Central: [PMC6558339](https://pubmed.ncbi.nlm.nih.gov/PMC6558339/)].
- Poplack SP, Tosteson TD, Kogel CA, Nagy HM. Digital breast tomosynthesis: initial experience in 98 women with abnormal digital screening mammography. *AJR Am J Roentgenol*. 2007;**189**(3):616-23. doi: [10.2214/AJR.07.2231](https://doi.org/10.2214/AJR.07.2231). [PubMed: [17751019](https://pubmed.ncbi.nlm.nih.gov/17751019/)].
- Helvie MA, Joynt LK, Cody RL, Pierce LJ, Adler DD, Merajver SD. Locally advanced breast carcinoma: Accuracy of mammography versus clinical examination in the prediction of residual disease after chemotherapy. *Radiology*. 1996;**198**(2):327-32. doi: [10.1148/radiology.198.2.8596826](https://doi.org/10.1148/radiology.198.2.8596826). [PubMed: [8596826](https://pubmed.ncbi.nlm.nih.gov/8596826/)].
- Rangarajan K, Hari S, Thulkar S, Sharma S, Srivastava A, Parshad R. Characterization of lesions in dense breasts: Does tomosynthesis help? *Indian J Radiol Imaging*. 2016;**26**(2):210-5. doi: [10.4103/0971-3026.184416](https://doi.org/10.4103/0971-3026.184416). [PubMed: [27413268](https://pubmed.ncbi.nlm.nih.gov/27413268/)]. [PubMed Central: [PMC4931780](https://pubmed.ncbi.nlm.nih.gov/PMC4931780/)].
- Kang DK, Jeon GS, Yim H, Jung YS. Diagnosis of the intraductal component of invasive breast cancer: Assessment with mammography and sonography. *J Ultrasound Med*. 2007;**26**(11):1587-600. doi: [10.7863/jum.2007.26.11.1587](https://doi.org/10.7863/jum.2007.26.11.1587). [PubMed: [17957053](https://pubmed.ncbi.nlm.nih.gov/17957053/)].
- Mercier J, Kwiatkowski F, Abrial C, Boussion V, Dieu-de Fraissinette V, Marraoui W, et al. The role of tomosynthesis in breast cancer staging in 75 patients. *Diagn Interv Imaging*. 2015;**96**(1):27-35. doi: [10.1016/j.diii.2014.06.010](https://doi.org/10.1016/j.diii.2014.06.010). [PubMed: [25086999](https://pubmed.ncbi.nlm.nih.gov/25086999/)].
- Meyers MO, Klauber-Demore N, Ollila DW, Amos KD, Moore DT, Drobish AA, et al. Impact of breast cancer molecular subtypes on locoregional recurrence in patients treated with neoadjuvant chemotherapy for locally advanced breast cancer. *Ann Surg Oncol*. 2011;**18**(10):2851-7. doi: [10.1245/s10434-011-1665-8](https://doi.org/10.1245/s10434-011-1665-8). [PubMed: [21442348](https://pubmed.ncbi.nlm.nih.gov/21442348/)].
- Wiechmann L, Sampson M, Stempel M, Jacks LM, Patil SM, King T, et al. Presenting features of breast cancer differ by molecular subtype. *Ann Surg Oncol*. 2009;**16**(10):2705-10. doi: [10.1245/s10434-009-0606-2](https://doi.org/10.1245/s10434-009-0606-2). [PubMed: [19593632](https://pubmed.ncbi.nlm.nih.gov/19593632/)].
- Jiang L, Ma T, Moran MS, Kong X, Li X, Haffty BG, et al. Mammographic features are associated with clinicopathological characteristics in invasive breast cancer. *Anticancer Res*. 2011;**31**(6):2327-34. [PubMed: [21737659](https://pubmed.ncbi.nlm.nih.gov/21737659/)].
- Liu S, Wu XD, Xu WJ, Lin Q, Liu XJ, Li Y. Is there a correlation between the presence of a spiculated mass on mammogram and luminal A subtype breast cancer? *Korean J Radiol*. 2016;**17**(6):846-52. doi: [10.3348/kjr.2016.17.6.846](https://doi.org/10.3348/kjr.2016.17.6.846). [PubMed: [27833400](https://pubmed.ncbi.nlm.nih.gov/27833400/)]. [PubMed Central: [PMC5102912](https://pubmed.ncbi.nlm.nih.gov/PMC5102912/)].
- Razzaghi H, Troester MA, Gierach GL, Olshan AF, Yankaskas BC, Millikan RC. Association between mammographic density and basal-like and luminal A breast cancer subtypes. *Breast Cancer Res*. 2013;**15**(5):R76. doi: [10.1186/bcr3470](https://doi.org/10.1186/bcr3470). [PubMed: [24008056](https://pubmed.ncbi.nlm.nih.gov/24008056/)]. [PubMed Central: [PMC3978452](https://pubmed.ncbi.nlm.nih.gov/PMC3978452/)].

20. Sartor H, Zackrisson S, Elebro K, Hartman L, Borgquist S. Mammographic density in relation to tumor biomarkers, molecular subtypes, and mode of detection in breast cancer. *Cancer Causes Control*. 2015;**26**(6):931-9. doi: [10.1007/s10552-015-0576-6](https://doi.org/10.1007/s10552-015-0576-6). [PubMed: [25860114](https://pubmed.ncbi.nlm.nih.gov/25860114/)].
21. Cai S, Yao M, Cai D, Yan J, Huang M, Yan L, et al. Association between digital breast tomosynthesis and molecular subtypes of breast cancer. *Oncol Lett*. 2019;**17**(3):2669-76. doi: [10.3892/ol.2019.9918](https://doi.org/10.3892/ol.2019.9918). [PubMed: [30867729](https://pubmed.ncbi.nlm.nih.gov/30867729/)]. [PubMed Central: [PMC6366033](https://pubmed.ncbi.nlm.nih.gov/PMC6366033/)].
22. Johnson K, Zackrisson S, Rosso A, Sartor H, Saal LH, Andersson I, et al. Tumor characteristics and molecular subtypes in breast cancer screening with digital breast tomosynthesis: The malmo breast tomosynthesis screening trial. *Radiology*. 2019;**293**(2):273-81. doi: [10.1148/radiol.2019190132](https://doi.org/10.1148/radiol.2019190132). [PubMed: [31478799](https://pubmed.ncbi.nlm.nih.gov/31478799/)].